The removal of basic dyes from aqueous solutions using agricultural by-products

Xue Song Wang [a,b,*], Yin Zhou [b], Yu Jiang [b], Cheng Sun [a]

[a] School of the Environment, Nanjing University, Nanjing, Jiangsu 210093, China
[b] Department of Chemical Engineering, Huaihai Institute of Technology, Lianyungang, Jiangsu 222005, China

Abstract

The adsorption of two basic dyes, namely, Malachite Green and Methylene Blue onto both agricultural by-products (i.e. rice bran and wheat bran) has been investigated in this study. The adsorption of both basic dyes was solution pH-dependent. The kinetic experimental data were analyzed using four kinetic equations including pseudo-first-order equation, pseudo-second-order equation, external diffusion model and intraparticle diffusion model to examine the mechanism of adsorption and potential rate-controlling step. The best-fit equation was identified using normalized standard deviation. The Langmuir and Freundich isotherms were used to fit the equilibrium data and the results showed that the Langmuir isotherm exhibited a little better fit to the Methylene Blue adsorption data by both adsorbents while the Freundlich isotherm seemed to agree better with the Malachite Green adsorption. The Gibbs free energy changes at 20 °C were calculated and the obtained values supported the conclusion that two dyes molecules adsorbed by physical processes. The effects of particle size, adsorbent concentration and solution ionic strength on the adsorption of the two basic dyes were also studied.
© 2008 Elsevier B.V. All rights reserved.

Keywords: Biosorption; Malachite Green; Methylene Blue; Equilibrium; Kinetic modeling

1. Introduction

Dyes are widely used in industries such as textiles, rubber, paper, plastics, cosmetics, etc. to color their products. There are more than 100,000 commercially available dyes with over 7×10^5 tonnes of dyestuff produced annually. It is estimated that 2% of dyes produced annually are discharged in effluent from manufacturing operations while 10% are discharged in effluent from textile and associated industries [1]. Basic dyes are the brightest class of soluble dyes used by the textile industry [2]. The release of dyes into waters by various industries poses serious environmental problems due to various dyes persistent and recalcitrant nature. Color in effluents can cause problems in several ways: dyes can have acute and/or chronic effects on exposed organisms depending on the expo-sure time and dye concentration; dyes are highly visible and undesirable even at very low concentrations in effluent; dyes absorb and reflect sunlight entering water and so can inter-fere with the growth of bacteria and hinder photosynthesis in aquatic plants; direct discharge of dyes containing efflu-ents into municipal wastewater plants and/or environment may cause the formation of toxic carcinogenic breakdown products [1]. Over 90% of some 4000 dyes tested in an ETDA (Eco-logical and Toxicological Association of the dyestuff) survey had LD_{50} values greater than 2000 mg/kg. The highest rates of toxicity were found amongst basic and diazo direct dyes [3]. In many developed countries such as the UK and EU countries, environmental policies have required that zero syn-thetic chemicals should be released into the marine environment [4].

Various techniques have been employed for the removal of dyes from wastewaters. These methods include adsorp-tion, nanofiltrtion, electrokinetic coagulation, coagulation and precipitation, advanced chemical oxidation, electrochemical oxidation, ozonation, supported liquid membrane, liquid–liquid extraction and biological process [5]. Robinson et al. [3] made a

* Corresponding author at: School of the Environment, Nanjing University, Nanjing, Jiangsu 210093, China. Tel.: +86 518 85895408;
fax: +86 518 85895409.

E-mail address: snowpine1969@yahoo.com.cn (X.S. Wang).

comprehensive review of various methods applied in removing the dye from textile wastewater.

The adsorption process is one of the efficient methods to remove dyes from effluent due to its low initial cost, simplicity of design, ease of operation and insensitivity to toxic substances [1]. Activated carbon is the most widely used adsorbent with great success due to its large surface area, micro-porous structure, high adsorption capacity, etc. However, its use is limited because of its high cost. This has led to search for cheaper substitutes [6]. A number of studies on the use of rice bran and wheat bran as adsorbents to remove heavy metals from aqueous solutions have been found in the literature [4]. But there are a limited number of studies related to some dyes adsorption on to rice bran and wheat bran. Earlier studies showed that untreated rice husk does not work for dyes of Congo Red, Sandolan blue, Sandolan rhodine, Solar blue and Foron blue, and has a low adsorption capacity for Foron brill red [4]. Hamdaoui and Chiha [2] made an investigation of adsorption kinetics of Methylene Blue from aqueous solutions by wheat bran and concluded that wheat bran is much economical, effective, viable, and can be an alternative to more costly adsorbents.

Malachite Green (MG) is a triphenyl methane dye, which is most widely used for coloring purpose, amongst all other dyes of its category. MG discharged into receiving waters even at low concentrations, will affect the aquatic life and cause detrimental effects in liver, gill, kidney, intestine and gonads. In humans, it may cause irritation to the gastrointestinal tract upon ingestion. Contact of MG with skin causes irritation, redness and pain [7].

Methylene Blue (MB) is also an important basic dye widely used for printing calico, dyeing, printing cotton and tannin and dyeing leather. Although not strongly hazardous, MB can have various harmful effects. The dye can cause eye burns, which may be responsible for permanent injury to the eyes of human and animals, irritation to the gastrointestinal tract with symptoms of nausea, vomiting and diarrhea and also cause methemoglobinemia, cyanosis, convulsions, tachycardia, and dyspnea. Contact of MB with skin causes irritation [2].

The aim of this study was to investigate the potential of using rice bran and wheat bran as low-cost adsorbents for the removal of the two basic dyes from aqueous solutions. The effects of solution pH, contact time, particle size, adsorbent concentration and ionic strength on both dyes removal efficiency were studied. Langmuir and Freundlich isotherms were employed to quantify the adsorption equilibrium. Four kinetic equations (pseudo-first-order equation, pseudo-second-order equation, external diffusion model and intraparticle diffusion model) were applied to investigate the adsorption mechanisms and potential rate-controlling step. These results will be useful for further application of both basic dyes in color removal of both dyes from wastewater.

2. Materials and methods

2.1. Adsorbent

The untreated rice bran and wheat bran were dried in an oven at 105 °C over a period of 24 h, and then ground and sieved to get two size fractions of 150–250 μm (denoted as coarse particle) and <150 μm (denoted as fine particle). Unless otherwise stated, the fine particles for both adsorbents were used for subsequent adsorption experiments.

2.2. Adsorbate

The adsorbates and their chemical structures (Fig. 1) utilized in this study are listed below. The dyestuffs were used as the commercial salts.

1. Methylene Blue (C.I. 52015, $\lambda_{max} = 663$ nm),
2. Malachite Green (C.I. 42000, $\lambda_{max} = 518$ nm).

2.3. Analytical techniques

The dyes were made up in stock solutions of concentration 1000 mg/L and were subsequently diluted to the required concentrations. Calibration curves for each dye were prepared by recording the adsorbance values for a range of known concentrations of dye solution at the wavelength to maximum adsorbance of each dye. The values of λ_{max} were used in all subsequent investigations using these dyes. All measurements were made on an UV/Vis spectrophotometer (UNICO-7200).

2.4. Experimental

Batch kinetic experiments were carried out at constant pH 6.0 with initial concentration of 80 mg/L and adsorbent concentration of 5 g/L at temperature of 20 °C. Samples were withdrawn at suitable time intervals by having them centrifuged.
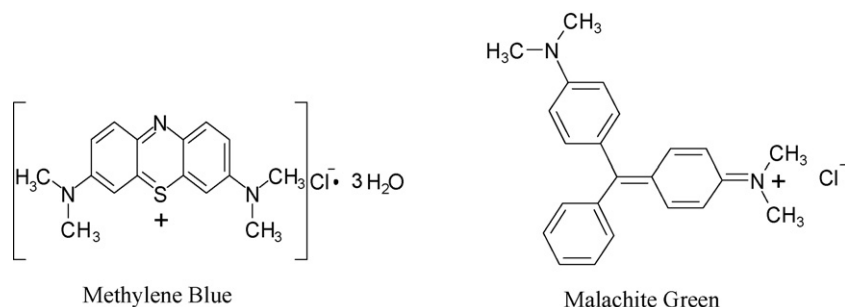

Fig. 1. Chemical structures of the utilized two dyes.

Batch equilibrium experiments were conducted using 125-mL conical flask at a total sample volume of 50 mL for each adsorption run. The samples were agitated in a reciprocating shaker to reach equilibrium. At the end of the reaction time, a known volume of the solution was removed and centrifuged for analysis of the supernatant.

The effect of pH on adsorption of adsorbate onto both adsorbents was investigated by varying the solution initial pH from 2.0 to 6.0. The effects of the adsorbent concentrations and the ionic strength of NaCl solution (0.05, 0.1, and 0.5 mol/L) on dye uptake were then examined. Temperature control was provided by the water bath shaker units. The solution pH was adjusted with strong acid (HCl) and/or strong base (NaOH) and recorded with a pH meter (PHS-3C).

2.5. Calculation

The amount of dye ions adsorbed at time t, q_t, was calculated from the mass balance equation

$$q_t = \frac{(C_0 - C_t)V}{m} \tag{1}$$

when time t (min) is equal to the equilibrium contact time, $C_t = C_e$, $q_t = q_e$, then the amount of dye ions adsorbed at equilibrium, q_e, was calculated using Eq. (1), where q_t and q_e (mg/g) are the amount of solute adsorbed onto the unit mass of the adsorbent at time t (min) and at equilibrium, respectively; C_0, C_t and C_e (mg/L) the concentration of the solute in the initial solution and in the aqueous phase at time t, and at equilibrium, respectively; V the solution volume (L) of the aqueous phase; and m (g) the amount of adsorbent used.

The removal efficiency was computed according to Eq. (2)

$$\text{Removal} \, (\%) = \frac{C_0 - C_e}{C_0} \times 100 \tag{2}$$

In order to quantitatively compare the applicability of different models, a normalized standard deviation, Δq, was calculated

$$\Delta q \, (\%) = 100 \times \sqrt{\frac{\sum [(q_{exp} - q_{cal})/q_{exp}]^2}{N - 1}} \tag{3}$$

where N is the number of data points, q_{exp} and q_{cal} (mg/g) the experimental and the calculated values of the equilibrium adsorbate solid concentration in the solid phase, respectively.

3. Theory

3.1. Equilibrium study

Equilibrium data, commonly known as adsorption isotherms, are basic requirements for the design of adsorption system. In adsorption isotherm study, adsorption isothermal equations usually utilized are Langmuir [8] and Freundlich [9] isotherms for the liquid–solid system.

The Langmuir isotherm

$$q_e = \frac{q_{max} b C_e}{1 + b C_e} \tag{4}$$

where q_{max} (mg/g) and b (L/mg) are Langmuir constants which are indicators of the maximum adsorption capacity and the affinity of the binding sites, respectively.

The Freundlich isotherm

$$q_e = k_f C_e^{1/n} \tag{5}$$

where k_f [(mg/g)/(mg/L)$^{1/n}$] and n (dimensionless) are the Freundlich constants, indicating adsorption capacity and adsorption intensity, respectively.

3.2. Kinetic study

In order to investigate the adsorption processes of two basic dyes on both adsorbents, four kinetic models (pseudo-first-order equation [10], pseudo-second-order equation [11], external diffusion sorption model [12] and intraparticle diffusion model [13]) were applied in this study.

The pseudo-first-order equation

$$\frac{dq_t}{dt} = k_1(q_{e,1} - q_t) \tag{6}$$

After definite integration by applying the initial boundary conditions $q_t = 0$ at $t = 0$ and $q_t = q_t$ at $t = t$, Eq. (6) becomes

$$q_t = q_{e,1}(1 - e^{-k_1 t}) \tag{7}$$

where k_1 (1/min) is the rate constant of pseudo-first-order model and $q_{e,1}$ (mg/g) the adsorption capacity at equilibrium.

The pseudo-second-order equation

$$\frac{dq_t}{dt} = k_2(q_e - q_t)^2 \tag{8}$$

On integration the pseudo-second-order Eq. (8) with boundary conditions $q_t = 0$ at $t = 0$ and $q_t = q_t$ at $t = t$ becomes

$$q_t = \frac{k_2 q_{e,2}^2 t}{1 + k_2 q_{e,2} t} \tag{9}$$

where k_2 (g/mg min) is the rate constant of pseudo-second-order model and $q_{e,2}$ (mg/g) the equilibrium adsorption capacity in this equation.

3.2.1. The external diffusion model

In the present study, the Spahn and Schlunder model [12] was chosen to describe the external diffusion on the adsorbent

$$\ln \frac{C_t}{C_o} = -k_{ext} t \tag{10}$$

where k_{ext} is the constant (1/min). If the Spahn and Schlunder model are applicable, the plot of $\ln C_t$ versus time t should give a linear relationship.

3.2.2. The Intraparticle diffusion model

Intraparticle diffusion model used here refers to the theory proposed by Weber and Morris [13]. The fractional approach to equilibrium varies according to a function of $(Dt^{0.5}/r^2)^{0.5}$, where r (m) is the particle radius and D (m^2/s) the diffusivity of solute within the particle [14]. The initial rate of intraparticle diffusion can be obtained by linearization of the curve

$$q_t = f(t^{0.5}) \tag{11}$$

Earlier studies have shown that such plot may present a multi-linearity, which indicates that two or more steps occur. The first, sharper portion is the external surface adsorption or instantaneous adsorption stage. The second portion is the gradual adsorption stage, where the intraparticle diffusion is rate-controlled. The third portion is final equilibrium stage where the intraparticle diffusion starts to slow down due to extremely low solute concentrations in the solution [14].

4. Results and discussion

4.1. Effect of initial solution pH

Previous studies have shown that the solution pH is the most important parameter affecting the cationic dye adsorption. Both dyes investigated in this study are basic in nature, which upon dissolution release colored dye cations into solution. The adsorption of these positively charged dye groups onto the adsorbent surface is primarily influenced by the surface charge on the adsorbent which in turn is influenced by the solution pH. The effect of initial solution pH on both dyes removal by two adsorbents is illustrated in Fig. 2. The result showed that availability of negatively charged groups at the adsorbent surface is necessary for the adsorption of basic dye to proceed, which at the highly acidic pH 2.0 is almost unlikely as there is a net positive charge in the adsorption system due to the presence of H_3O^+. In such a system H^+ competed with dye cations, resulting in active sites to become protonated to the exclusion of dye cations binding on the adsorbent surface. In contrast, as the pH increased, more negatively charged surface was available thus facilitating greater dye cations removal.
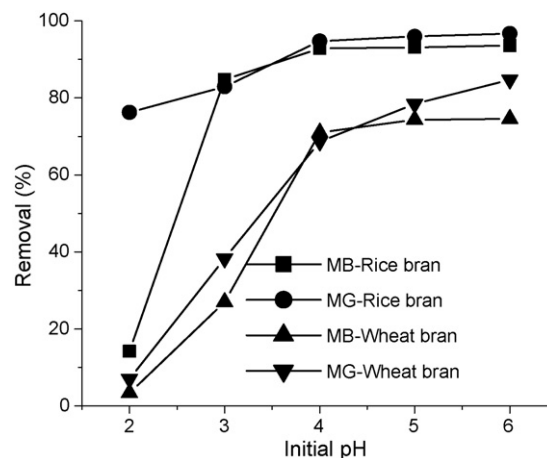

Fig. 2. Effect of the initial solution pH on the removal of basic dyes by both adsorbent of fine particle size (temperature 20 °C; adsorbent concentration 5 g/L; initial dye concentration 80 mg/L; contact time 120 min).

4.2. Kinetics of adsorption

Fig. 3 shows the adsorption kinetics of basic dyes by both the dye uptake capacity, q_t, versus time at the initial dye concentration of 80 mg/L. A larger amount of dyes was removed in the first 20–30 min of contact time and equilibriums were established in 60–90 min for both adsorbents. The rapid kinetics has significant practical importance as it will facilitate smaller reactor volumes ensuring efficiency and economy [15]. Increasing the particle size increased both dyes removal by wheat bran but decreased by rice bran. This may likely be ascribed to the difference in the structure and chemical composition of both adsorbents. The time profile of basic dyes adsorption is a single, smooth, and continuous curve leading to saturation, suggesting the possible monolayer coverage of dye on the surface of the adsorbent [2]. In the subsequent experiments, contact time of 120 min was chosen to ensure to attain adsorption equilibrium.

In order to examine the mechanism of adsorption and potential rate-controlling step such as mass transfer and chemical reaction processes, several kinetic models were applied to test experimental data.
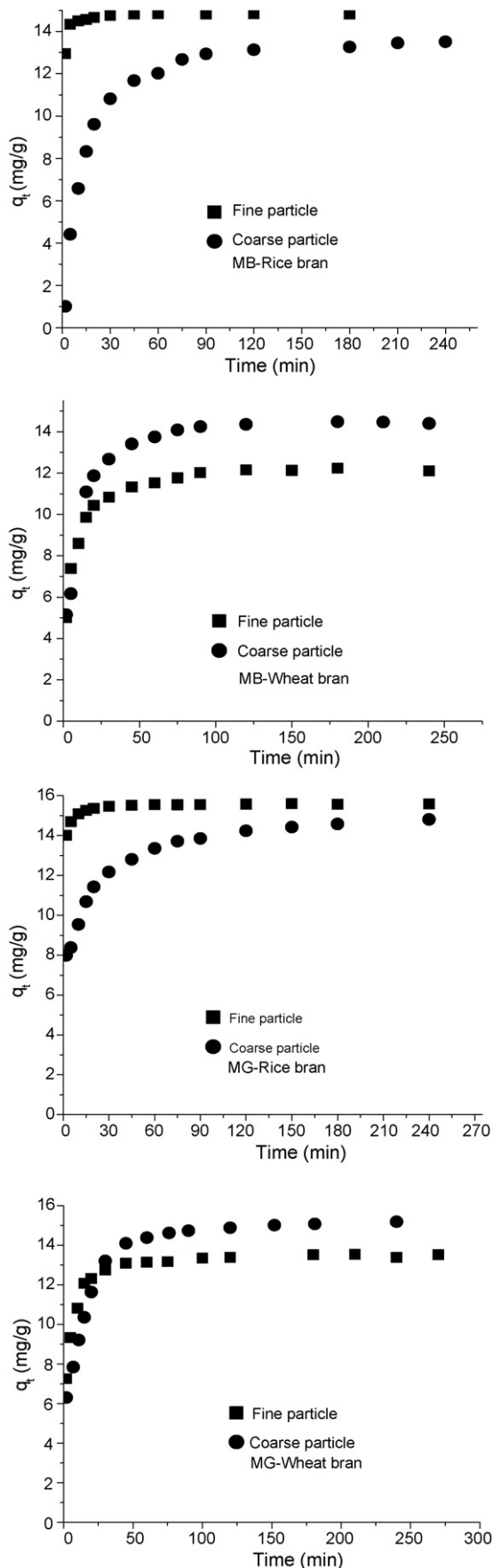
Table 1
The values of kinetic parameters for pseudo-first-order equation and pseudo-second-order equation together with normalized standard deviations (temperature 20 °C; adsorbent concentration 5 g/L; initial concentration 80 mg/L; pH 6.0)

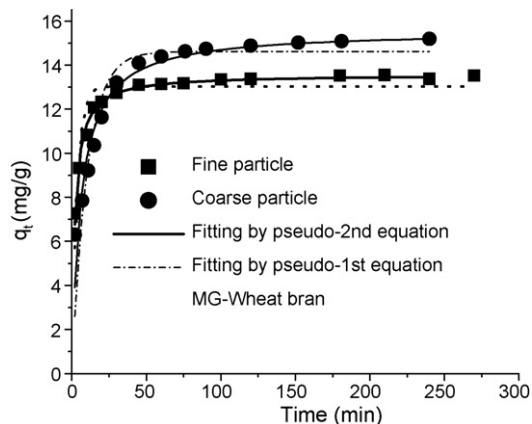| Adsorbent/adsorbate	Pseudo-first-order			Pseudo-second-order		
	$q_{e,1}$ (mg/g)	k_1 (1/min)	Δq (%)	$q_{e,2}$ (mg/g)	k_2 (g/mg min)	Δq (%)
Rice bran						
MB fine particle	14.7056	1.0544	1.03	14.8944	0.2379	0.61
Coarse particle	12.9706	0.0666	17.75	14.3720	0.0062	32.16
MG fine particle	15.4152	1.1767	1.61	15.5674	0.2669	0.46
Coarse particle	13.3339	0.1974	16.23	14.1309	0.0229	10.32
Wheat bran						
MB fine particle	11.6039	0.1770	10.56	12.2935	0.02356	3.43
Coarse particle	13.9836	0.1163	13.14	14.9359	0.01254	7.85
MG fine particle	13.0439	0.2764	7.94	13.5700	0.03667	2.42
Coarse particle	14.6106	0.0976	16.98	15.5616	0.01079	11.32

Fig. 4. Typical plots of comparison between the measured and modeled time profiles for adsorption of MB onto the two particle sizes of wheat bran (temperature 20 °C; adsorbent concentration 5 g/L; initial dye concentration 80 mg/L; pH 6.0).

Table 1 presents the results of fitting experimental data with pseudo-first-order and pseudo-second-order equations using non-linear analysis. As seen from Table 1, the order of Δq (%) was pseudo-first-order equation > pseudo-second-order equation, indicating the experimental data conformed better to the pseudo-second-order equation except for the system of MB adsorption on to rice bran of coarse particle. Fig. 4 typically illustrates the comparison between the calculated and measured results for the adsorption of MG on to wheat bran of two particle sizes. It is found that the pseudo-first-order equation overestimates at the initial stage of adsorption and underestimates at the final stage while the pseudo-second-order equation predicts the behavior over the "whole" range of studies strongly supporting its validity.

Adsorption, whether physical or chemical, involves the mass transfer of a soluble species (adsorbate) from bulk solution to the surface of a solid phase (adsorbent). When the adsorbent is a porous media, the transport of adsorbate to adsorbent will occur through four main steps [17–19]:

Bulk solution transport: the adsorbate is first transported from the bulk solution to the hydrodynamic boundary layer surrounding the adsorbent.

External (film) resistance to transport (external diffusion): the adsorbate must then pass through the hydrodynamic layer to the surface of the adsorbent. Transportation through the boundary layer is due to molecular diffusion, and the distance the adsorbate must travel, or the thickness of the boundary layer, will depend on the velocity of the bulk solution. The size of the boundary layer will affect the rate of transportation. The thinner the boundary layer, the higher the rate of the transportation.

Internal (pore) transport (intraparticle diffusion): this step occurs after the adsorbate has passed through the boundary layer and must be transported through the pores to adsorption sites. This intraparticle transportation may occur by molecular diffusion through the solution in the pores (pore diffusion) or by diffusion along the adsorbent surface (surface diffusion) after adsorption takes place.

Fig. 3. Time profiles of adsorption of basic dyes onto two particle sizes of both adsorbents (temperature 20 °C; adsorbent concentration 5 g/L; initial dye concentration 80 mg/L; pH 6.0).
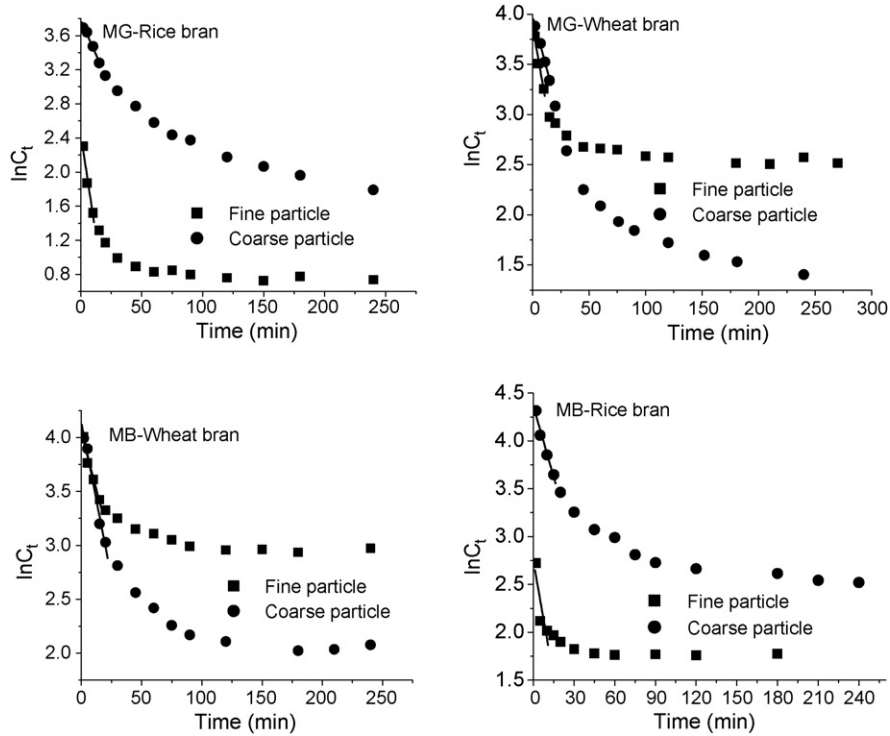
Fig. 5. Test of external diffusion model for adsorption of basic dyes for two particle sizes on to both adsorbents (temperature 20 °C; adsorbent concentration 5 g/L; initial dye concentration 80 mg/L; pH 6.0).

Adsorption: the final step is the attachment of the adsorbate onto the adsorbent surface at available sites. This step is very rapid; therefore one of the preceding diffusion steps will control the rate of mass transfer.

It is essential to understand these mass transfer mechanisms in order to design a cost effective and efficient adsorption system. Bulk transportation and adsorption are rarely, if ever, rate-limiting steps [18]. The transportation mechanisms of concern,
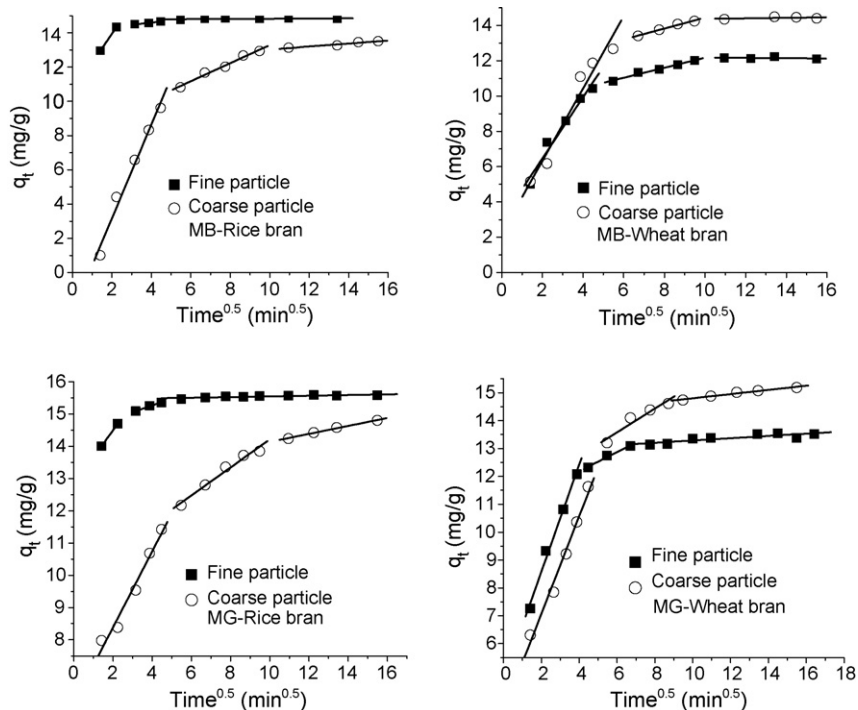

Fig. 6. Test of intraparticle diffusion model for adsorption of basic dyes for two particle sizes on to both adsorbents (temperature 20 °C; adsorbent concentration 5 g/L; initial dye concentration 80 mg/L; pH 6.0).

Table 2
The values of rate parameters of different stages for intraparticle diffusion equation (temperature 20 °C; adsorbent concentration 5 g/L; initial concentration 80 mg/L; pH 6.0)

Adsorbent/adsorbate	$k_{p,1}$ (mg/g min$^{0.5}$)	$k_{p,2}$ (mg/g min$^{0.5}$)	$k_{p,3}$ (mg/g min$^{0.5}$)	Δq (%)
Rice bran				
MB fine particle	1.6844	0.1248	0.0054	0.1137
Coarse particle	2.7405	0.5282	0.0895	1.0747
MG fine particle	0.8536	0.2076	0.0105	0.109
Coarse particle	1.1768	0.4344	0.1235	0.6048
Wheat bran				
MB fine particle	1.7347	0.2834	0.0087	1.0049
Coarse particle	2.0504	0.3104	0.0150	3.2225
MG fine particle	1.9210	0.3438	0.0409	0.4545
Coarse particle	1.7528	0.4279	0.0749	0.8199

therefore, are external film diffusion and intraparticle diffusion. If the adsorption process is controlled by the external resistance, the plot of ln C_t versus time should be linear. This kind of relation was indicated for the initial stages (<15 min) of adsorption kinetics of the two dyes by both adsorbents used (Fig. 5), which suggests that the external diffusion was the rate-controlling step of the initial fast adsorption of both dyes onto adsorbents. This is in agreement with the results obtained by Hamdaoui and Chiha [2], who investigated the removal of MB from aqueous solutions by wheat bran.

Plots of basic dyes amounts adsorbed, q_t versus $t^{0.5}$, are presented for the two particle sizes of adsorbents in Fig. 6. It is clearly found that adsorption of basic dyes onto the two particle sizes of adsorbents followed three stages: an instantaneously extremely fast uptake, a transition stage and an almost flat plateau portion. Stage 1 is attributed to the instantaneous utilization of the most readily available sites on the adsorbent external surface. Stage 2, exhibiting additional removal, is ascribed to the intraparticle diffusion, stimulating further migration of adsorbate from the liquid phase to the adsorbent internal surface. Stage 3, the plateau section shows the final equilibrium state. The slope of the lines in each stages is termed as the rate parameter $k_{p,i}$ (i = stage number). Rate parameters of the different stages are listed in Table 2. As seen from the table, the order of adsorption rate was the first stage ($k_{p,1}$) > second stage ($k_{p,2}$) > third stage ($k_{p,3}$). As mentioned above, initially, the dye was adsorbed by the external surface of the adsorbent, so the adsorption rate was very

fast. When the adsorption of the external surface reached saturation, the dye molecule entered into the pores within the particle and eventually was adsorbed on the active sites of the adsorbent internal surface. When the dye molecule transported in the pore of the particle, the diffusion resistance increased and consequently reduced the diffusion rate. With the decrease of the dye concentration in the solution, the diffusion rate became much smaller and the diffusion processes reached the final equilibrium stage [19].

Table 2 also shows the effect of particle size on diffusion rates of different stages. The larger the particle size, the faster the dye molecule diffused. This is in agreement with the result obtained by Sun and Yang [16], who investigated the adsorption of basic dyes from aqueous solution on modified peat-resin particle.

4.3. Effect of adsorbent concentration

Fig. 7 shows the adsorption of both dyes investigated as a function of adsorbent concentrations for both adsorbents in a solution of pH 6.0. It is found that by increasing the adsorbent concentrations the removal efficiency increased but adsorption capacity (i.e. adsorption amount per unit mass) decreased. This can be attributed the fact that the number of available adsorption sites increased by an increase in adsorbent and this therefore resulted in an increase in removal efficiency. The decrease in adsorption capacity with an increase in the adsorbent concentration could be ascribed to the fact that some of the adsorption sites

Table 3
The values of isothermal parameters for the Langmuir and Freundlich equations together with the normalized standard deviations and Gibbs free energy change (temperature 20 °C; adsorbent concentration 5 g/L; pH 6.0; contact time 120 min)

| Adsorbent/adsorbate	Langmuir			Freundlich			$-\Delta G$ (kJ/mol)
	q_{max} (mg/g)	b (L/mg)	Δq (%)	k_f [(mg/g)/(mg/L)$^{1/n}$]	n (–)	Δq (%)	
Rice bran							
MB fine particle	54.9933	0.06229	4.4560	8.9698	2.6478	29.0819	33.6
Coarse particle	20.2931	0.13666	4.4958	7.1575	4.7449	18.9330	35.5
MG fine particle	68.9719	0.09657	12.0750	8.2553	1.6796	5.5335	35.0
Coarse particle	38.4774	0.05993	11.9001	5.5158	2.4005	10.3429	33.8
Wheat bran							
MB fine particle	16.6282	0.08872	12.1263	6.1945	5.5886	22.2903	34.4
Coarse particle	54.7874	0.03727	8.1312	6.1872	2.3224	18.6846	32.3
MG fine particle	66.5743	0.01740	7.8836	2.3664	1.5287	7.3765	30.8
Coarse particle	75.6487	0.03679	9.1682	4.5692	1.5685	9.4862	32.6
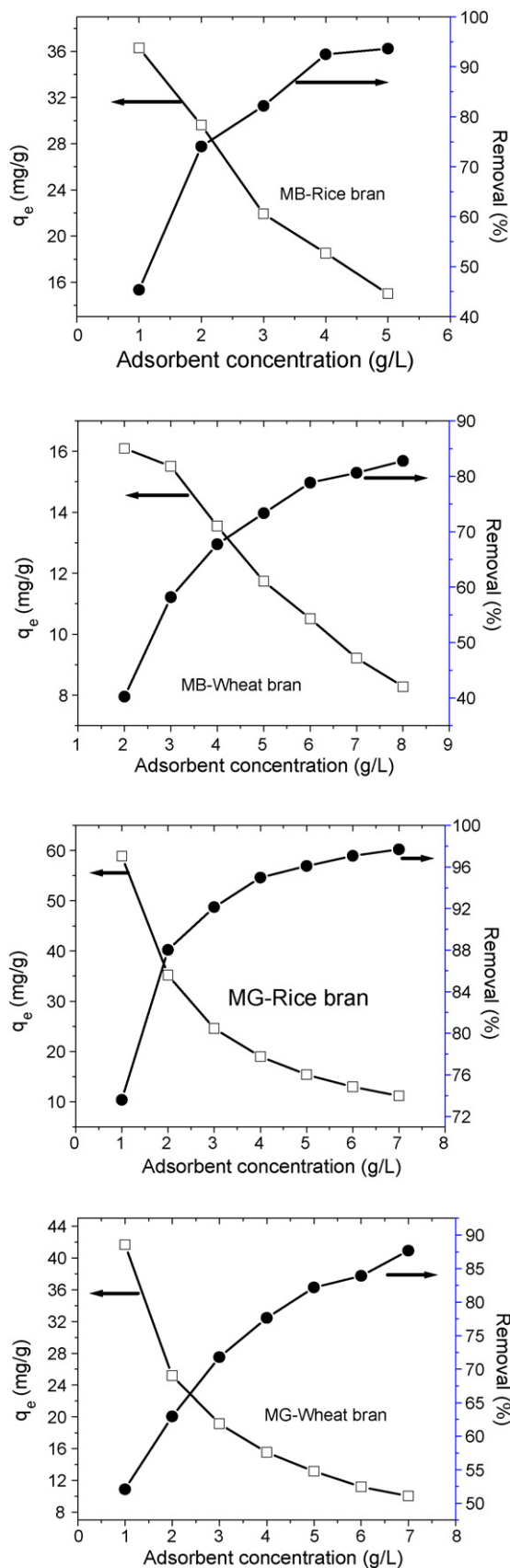
Fig. 7. Effect of adsorbent concentration on the basic dyes of adsorption (temperature 20 °C; initial dye concentration 80 mg/L; pH 6.0; contact time 120 min).

remained unsaturated during the adsorption process. Another reason could likely be due to the inter-particle interaction, such as aggregation, resulting from high adsorbent concentration. Such aggregation would lead to a decrease in the total surface area of the adsorbent and an increase in the diffusion path length [20].

4.4. Equilibrium modeling

Analysis of equilibrium data is of importance for developing an equation that can be used for design purposes. The Langmuir and Freundlich adsorption isotherms for two particle sizes of both adsorbents at a temperature of 20 °C are given in Figs. 8 and 9. The Langmuir and Freundlich adsorption constants evaluated from the isotherms together with the normalized standard deviations are presented in Table 3. In point of the numerical values of normalized standard deviation in the table, the Langmuir isotherm exhibited a little better fit to the MB adsorption data by both adsorbents while the Freundlich isotherm seemed to agree better with MG adsorption.

An adsorption isotherm is characterized by certain constants the values of which express the surface properties and affinity of the adsorbent and can also be used to find the maximum adsorption capacity. Table 3 shows that the value of n is greater than unity, indicating both basic dyes were favorably adsorbed by both adsorbents. The maximum adsorption capacity (q_{max}) increased with the decreasing particle size of rice bran for both adsorbate but with the increasing particle size of wheat bran.

The apparent free energy change of adsorption, ΔG (kJ/mol), at 20 °C was calculated and also listed in Table 3 using the following equation

$$\Delta G = -RT \ln 55.5b' \tag{12}$$

where b' is the Langmuir constant when the concentration term is expressed in L/mol, R the ideal gas constant (8.314 J/mol K), T the absolute temperature (K), the value of 55.5 is the concentration of water in solution expressed in mol/L.

As seen from Table 3, the negative value of ΔG indicates the spontaneous adsorption of dye molecules, which is usually characteristic for strong interaction with adsorbent surface. Moreover, the values of ΔG are more positive than −40 kJ/mol, which indicate physical adsorption process [21].

4.5. Effect of ionic strength

Dye-laden wastewaters released from different industries contain various types of salts. The presence of these salts leads to high ionic strength, which may significantly affect the performance of the adsorption process. Fig. 10 shows clearly that the variation of sodium chloride concentration exhibits a major effect on the extent of both basic dyes adsorption.

That the extent of adsorption is sensitive to changes in concentration of supporting electrolyte (chloride sodium) indicates that electrostatic attraction may be a significant component of the overall adsorption in this system. The electrostatic free energy change, ΔG_{elect}, contributes to the total free energy change of
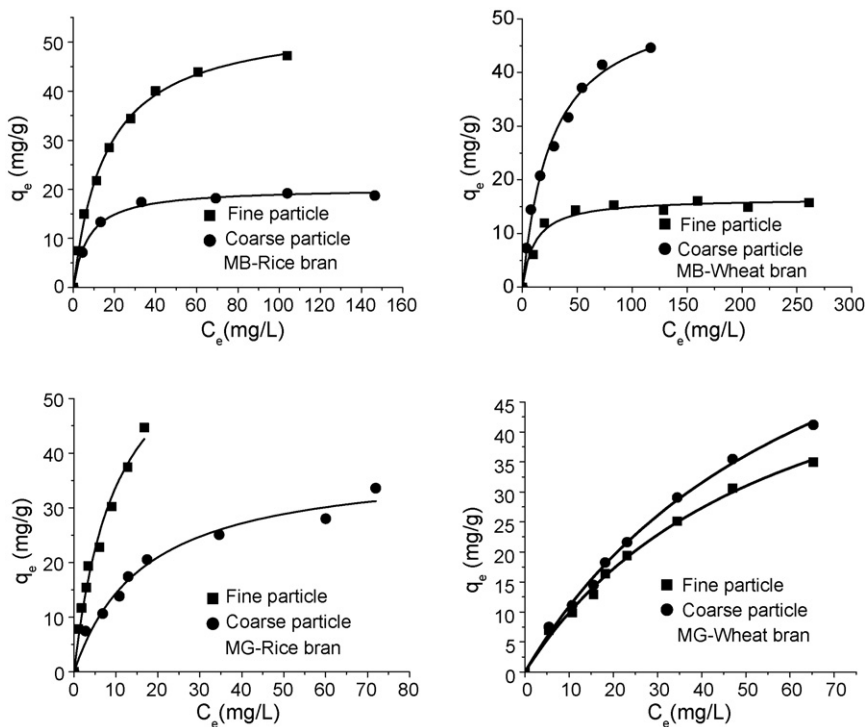
Fig. 8. The Langmuir adsorption isotherms of basic dyes on to two particle sizes of both adsorbents (temperature 20 °C; adsorbent concentration 5 g/L; pH 6.0; contact time 120 min).

adsorption, ΔG, and depends on the ionic strength of solution. This term is given as [22]

$$\Delta G_{\text{elect}} = zF\psi_d \qquad (13)$$

where z represents the ionic charge, F the Faraday constant (96487C) and Ψ_d the potential in the plane of the adsorbed ion.

When the ionic strength was increased, the electrical double layer surrounding the adsorbent surface was compressed, which
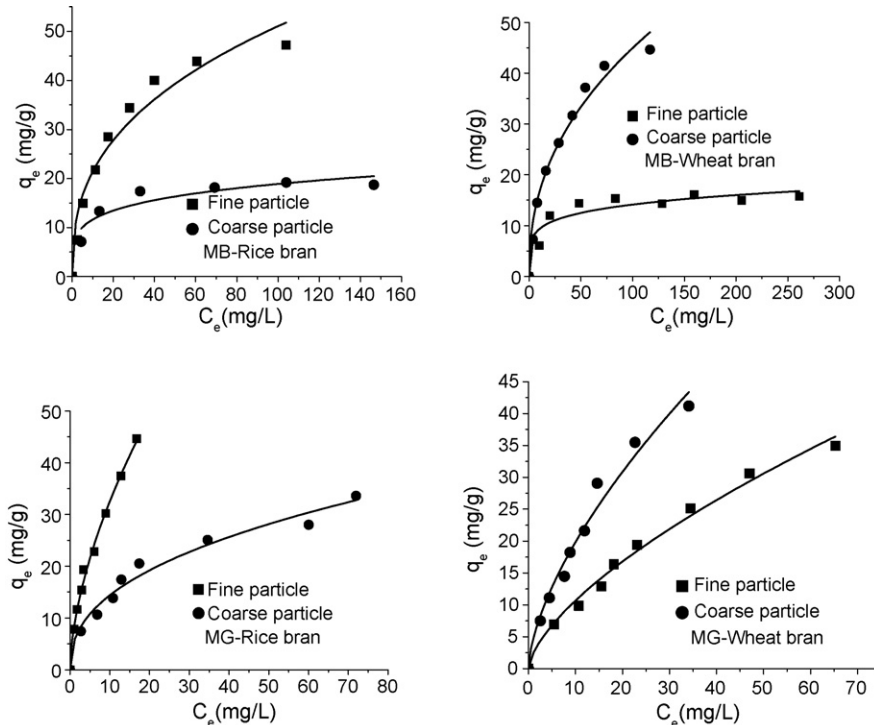

Fig. 9. The Freundlich adsorption isotherms of basic dyes on to two particle sizes of both adsorbents (temperature 20 °C; adsorbent concentration 5 g/L; pH 6.0; contact time 120 min).
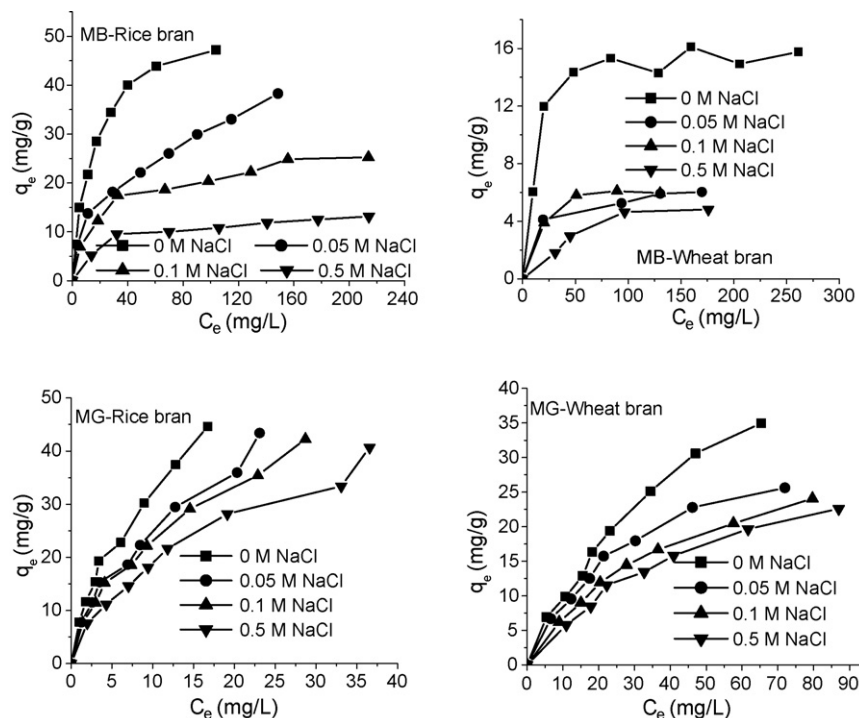
Fig. 10. Effect of ionic strength on adsorption of dye molecules onto adsorbents (temperature 20 °C; adsorbent concentration 5 g/L; pH 6.0; contact time 120 min).

would lead to a decrease in the electrostatic potential, Ψ_d. This indirectly resulted in a reduction in the coulombic free energy, and a decrease in basic dye ions adsorption.

In an attempt to quantify the ionic strength effects, three competitive modes were examined, which may be useful in helping to describe the seemingly "inhibitory" effect of increasing chloride sodium concentrations on the basic dye adsorption. These three modes are described below and illustrated in Fig. 11.

4.5.1. Competitive mode

According to the competitive mode, the sodium ions interact directly with the active sites on the adsorbent surface, competing with basic dye for the available sites. For the competitive isotherm, the intercept term of the linearized Langmuir isotherms remains constant.

4.5.2. Uncompetitive mode

For uncompetitive inhibition, the sodium ions do not react with the active sites on the adsorbent surface directly, but instead react with the adsorbent surface-dye complexes. In this case, the linearized Langmuir adsorption isotherms remain parallel to each other.

4.5.3. Noncompetitive mode

This mechanism is a combination of the above two modes. Both the sodium ions and basic dye adsorb independently at different sites on the adsorbent surface. In other words, sodium ions react with the adsorbent surface sites and dye molecules-adsorbent surface complexes, while dye molecules react with the adsorbent surface active sites and sodium ions-adsorbent sur-

face complexes. In this case, the linearized Langmuir isotherms converge at x-axis.

In examining the reciprocal plots of Fig. 12, it appears that the sodium ion acted as a competitive inhibitor during the adsorption process.
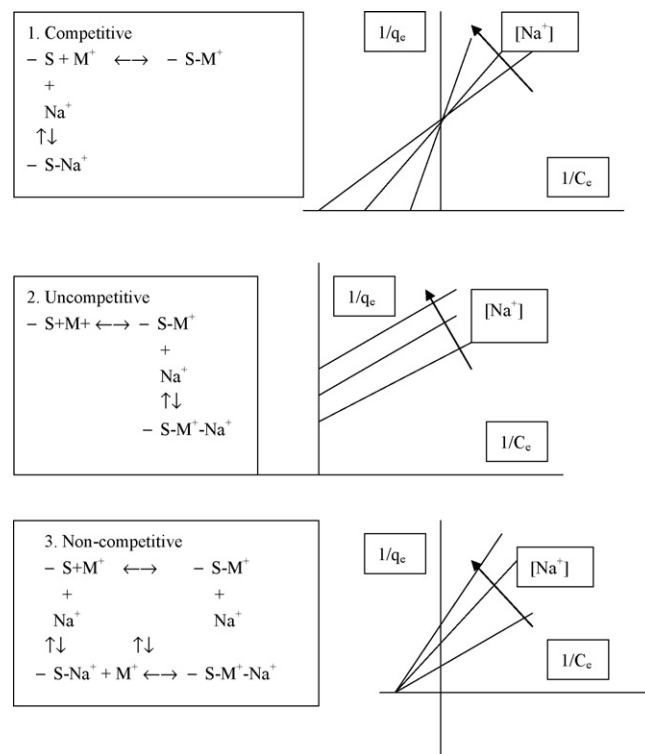

Fig. 11. Schematic of variations of linearized Langmuir isotherms. (The sign of "—S" represents the active sites of the adsorbent surface used in this study.)
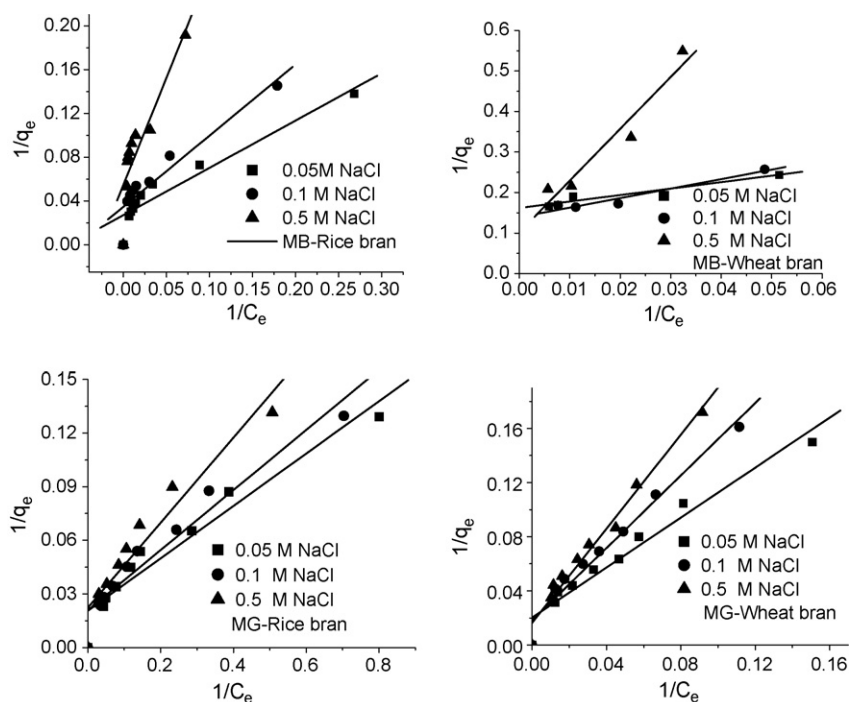
Fig. 12. The reciprocal plots for the effect of ion strength on the dye ions adsorption (temperature 20 °C; adsorbent concentration 5 g/L; pH 6.0; contact time 120 min).

5. Conclusions

The adsorption of two basic dyes on to both agricultural by-products was investigated in batch experimental system. The following results were obtained:

1. The solution pH played a significant role in influencing the capacity of both adsorbents towards two basic dyes. An increase in the pH of solution would lead to a significant increase in the adsorption capacity.
2. The adsorbed amounts of two basic dyes increased with an increase in contact time and reached equilibrium in 60–90 min. The experimental data conformed better to the pseudo-second-order equation. The external diffusion was the rate-controlling step of the initial fast adsorption (<15 min) and in the next stage the intraparticle diffusion dominated the mass transfer process.
3. The Langmuir isotherm exhibited a little better fit to the MB adsorption data by both adsorbents while the Freundlich isotherm seemed to agree better with the MG adsorption. Thermodynamic analysis revealed that the adsorption behaviors of two basic dyes could be considered as a spontaneous and physical process.
4. The removal efficiency increased and the adsorption capacity decreased with a rise in adsorbent concentrations.
5. The adsorption capacity of both adsorbents towards the two basic dyes decreased with an increase in ionic strength.
6. The adsorption of two basic dyes by both adsorbents was particle-size dependent.

References

[1] S.J. Allen, B. Koumanova, Decolourisation of water/wastetwater using adsorption, J. Univ. Chem. Technol. Metallurgy 40 (2003) 175–192.
[2] O. Hamdaoui, M. Chiha, Removal of methylene blue from aqueous solutions by wheat bran, Acta Chim. Slov. 54 (2007) 407–418.
[3] T. Robinson, G. McMullan, R. Marchant, P. Nigam, Remediation of dyes in textile effluent: a critical review on current treatment technologies with a proposed alternative, Bioresour. Technol. 77 (2001) 247–255.
[4] T.G. Chuah, A. Jumasiah, I. Azni, S. Katayon, S.Y. Thomas Choong, Rice husk as a potentially low-cost biosorbent for heavy metal and dye removal: an overview, Desalination 175 (2005) 305–316.
[5] A.S. Mahmoud, A.E. Ghaly, M.S. Brooks, Removal of dye from textile wastewater using plant oils under different pH and temperature conditions, Am. J. Environ. Sci. 3 (2007) 205–218.
[6] P.K. Malik, Use of activated carbons prepared from sawdust and rice husk for adsorption of acid dyes: a case study of acid yellow 36, Dyes Pigments 56 (2003) 239–249.
[7] N. Daneshvar, M. Ayazloo, A.R. Khataee, M. Pourhassan, Biological decolorization of dye solution containing Malachite Green by microalgae Cosmarium sp., Bioresour. Technol. 98 (2007) 1176–1182.
[8] I. Langmuir, The adsorption of gases on plane surfaces of glass, mica and platinum, J. Am. Chem. Soc. 40 (1918) 1361–1403.
[9] H. Freundlich, Udber die adsorption in Loesungen, Z. Physik. Chem. 57 (1907) 385–470.
[10] S. Lagergren, Zur theorie der sogenannten adsorption gelöster stoffe, Kungliga Svenska Vetenskapsakademiens Handlingar 24 (1898) 1–39.
[11] Y.S. Ho, J.C.Y. Ng, G. McKay, Kinetics of pollutant sorption by biosorbents: review, Sep. Purif. Methods 29 (2000) 189–232.
[12] H. Spahn, U. Schlunder, The scale-up of activated carbon columns for water purification, based on results from batch tests: part I, Chem. Eng. Sci. 30 (1975) 529–537.
[13] W.J. Weber Jr., J.C. Morris, Kinetics of adsorption on carbon from solution, J. Sanit. Eng. Div. ASCE 89 (1963) 31–59.
[14] F.C. Wu, R.L. Tseng, R.S. Juang, Kinetic modeling of liquid-phase adsorption of reactive dyes and metal ions on chitosan, Wat. Res. 35 (2001) 613–618.

[15] Z. Asku, Equilibrium and kinetic modeling of cadmium (II) biosorption by *C. vulgaris* in a batch system: effect of temperature, Sep. Purif. Technol. 21 (2001) 285–294.

[16] Q. Sun, L. Yang, The adsorption of basic dyes from aqueous solution on modified peat-resin particle, Water Res. 37 (2003) 1535–1544.

[17] S. Mortazavi, F. Tezel, A.Y. Tremblay, K. Volcheck, Effect of pH on the uptake of arsenic from contaminated water by activated alumina, Adv. Environ. Res. 3 (1999) 103–118.

[18] G. Prasad, Removal of arsenic (V) from aqueous systems by adsorption onto some geological materials, in: J.O. Nriagu (Ed.), Aquatic Surface Chemistry—Chemical Processes at the Particle-Water Interface, John Wiley & Sons, Inc., 1994, pp. 133–154.

[19] V.L. Snoeyink, R.S. Summers, Adsorption of organic compounds, Water Quality and Treatment: A Handbook of Community Water Supplies, fifth ed., MiGraw-Hill Inc., 1999.

[20] S.S. Reddy, B. Kotaiah, N.S.P. Reddy, M. Velu, The removal of composite reactive dye from dyeing unit effluent using sewage sludge derived activated carbon, Turkish J. Eng. Env. Sci. 30 (2006) 367–373.

[21] H.M.A. Soliman, H.H. Abdel-Rahman, The use of rotating cylinder electrode to study the effect of 1,3-dihydroxypropane on the production of copper powder, J. Braz. Chem. Soc. 17 (2006) 705–714.

[22] C.P. Huang, E.H. Smith, Removal of Cd (II) from plating wastewater by an activated carbon process, in: W.J. Cooper (Ed.), Chemistry in Water Reuse, 2, Ann Arbor Science Publishers, Inc., Michigan, 1981, pp. 355–400.